https://doi.org/10.48048/tis.2024.8358

Effect of CCl_4 on Renal Tissues of Male Mice and Prevented by Pretreatment with Bromelain Loaded with Gold Nanoparticles: Histopathological and Caspase-9 Expression Alterations

Haneen Ibrahim Ali[1,2,*], Baydaa Hussain Mutlak[1], Sohad Abdulkaleg Alshareef[3] and Zamzam Alhuwaymil[4]

[1]Department of Biology, College of Education for Pure Science, Ibn Al-Haitham, University of Baghdad, Baghdad, Iraq
[2]College of Dentistry, Al-Iraqi University, Baghdad, Iraq
[3]Department of Chemistry, Faculty of Science, University of Tabuk, Tabuk, Saudi Arabia
[4]Organic Department, College of Science and Humanites at Al-Quway'iyah, Shaqra University, Shaqra, Saudi Arabia

([*]Corresponding author's e-mail: haneen.i.ali@aliraqia.edu.iq)

Received: 27 April 2024, Revised: 28 May 2024, Accepted: 4 June 2024, Published: 25 October 2024

Abstract

The study aimed to investigate the potential protective effect of bromelain on renal histopathological changes induced by carbon tetrachloride (CCl_4) in albino mice. CCl_4 is widely used in the chemical industry but is also known to cause toxicity to various organs including the brain, liver, kidneys and lungs. In this study, 49 animals were divided into 7 equal groups. The kidneys of the mice were examined to assess histopathological changes and immunohistochemical markers, specifically caspase-9. The groups that received bromelain solution coated with gold nanoparticles demonstrated greater protective effects against CCl_4-induced kidney damage. The findings suggest that kidney damage induced by CCl_4 may be attributed to oxidative stress, which disrupts the antioxidant defense system, enzyme function and biochemical markers. However, administration of bromelain significantly mitigated CCl_4 toxicity by enhancing the antioxidant defense system and reducing the production of free radicals. Notably, the study found that a dose of 300 mg of bromelain effectively reduced CCl_4-induced toxicity in rats. This highlights the potential therapeutic value of bromelain in protecting against chemical-induced kidney damage.

Keywords: Kidney, Gold nanoparticles, Bromelain, Antioxidant, Anti-inflammatory, Histopathological, Immunohistochemical

Introduction

Carbon tetrachloride (CCl_4) belongs to a group of well-known organic compounds called (alkyl halides) [1]. The kidneys are among the important organs that are exposed to toxicity with this compound, and this toxicity causes multiple damages after a few days of exposure, including inflammation and fibrosis of the nephrons, kidney failure and a decrease or absence of urine. After this compound damages the liver, kidney failure occurs immediately after the 2nd week of exposure. This exposure is also accompanied by protein, sugar and hemoglobin in the urine, and its appearance may cause high blood pressure and acidity [2,3]. Numerous plants, including the Bromeliaceae family's *Ananas comosus* (pineapple), are of great interest due to their potential as antioxidants. *Ananas comosus* is mostly grown in equatorial areas around

the world and is recognized to have a variety of beneficial health advantages, including anti-inflammatory, anti-cancer and anti-platelet properties. The inexpensive byproduct waste of *Ananas comosus* is rich in complex enzymes identified by bromelain, which are crucial for several clinical applications, including wound healing, tumor growth modulation, anti-inflammatory, anti-diarrhea and digestive aid [4-6]. According to Manosroi *et al.* [7], bromelain possesses antioxidant qualities that enable it to scavenge free radicals and stop lipids from oxidizing. Bromelain contains a variety of protease inhibitors, cellulases, glycoproteins, phosphatases, glucosidase, peroxidases and thiol endopeptidases [8,9]. To develop a material that prevents degenerative illnesses, it is important to determine antioxidative activity [10]. A quick and easy method to measure the antioxidant activity of bromelain was to compare its results against the 1,1-diphenyl-2-picrylhydrazyl radical [11,12].

Just as important as the therapeutic agent selection is how the drug is delivered to the targeted tissues and cells. The utilization of nanoparticles offers several benefits, particularly in the medical area, despite the ongoing argument over their cytotoxicity [13]. Due to their special properties, including their small sizes and large surface areas relative to their size, as well as their ability to readily pass through biological membranes and barriers to reach hard-to-reach areas, nanoparticles of many types have been used recently as carriers that aid in the delivery of therapeutic materials [14].

Apoptotic induction is mostly dependent on caspases, which are proteases belonging to the interleukin-1β-converting enzyme family. Select caspases function as either effector (caspase-3, -6 and -7) or initiators (caspase-1, -2, -4, -5, -8, -9 and -10) [15]. The intrinsic or extrinsic route mediates apoptosis in animals. The intrinsic pathway is triggered by cellular stress and activates caspase-9, whereas the extrinsic pathway is started by ligation of death receptors and activates caspase-8. In these pathways, caspase-3 is a downstream effector protease [16].

The study's objectives are to improve the damage caused by carbon tetrachloride poisoning, which is known for its toxicity, and to develop a dosage technique that relies on loading bromelain on gold nanoparticles to increase the enzyme's availability in the body and ensure an increase in effectiveness. Despite the numerous benefits of bromelain, as evidenced by studies and research, its effectiveness is limited, as is the case with all plant extracts, due to its low bioavailability in the body.

Materials and methods

Materials and reagents

Carbon tetrachloride, trisodium citrate, bromelain (EC:3.4.22.32) and chloroauric trihydrate (HauCl4.3H2O) were acquired from Sigma-Aldrich (St. Louis, USA). Only reagents of the analytical grade are used. DIW, or de-ionized water, was used for all reaction and laboratory requirements.

Preparation of the AuNPs and Br-AuNPs

They are mixing 1.0 g of HAuCl4. 3H2O with 250 mL of pure water yields a 10.0 mM stock solution of gold(III) ions. To get the 1.0 mM concentration needed for this experiment, dilute 25 mL of stock with 250 mL. The gold solution (Stoke) was diluted to a concentration of 1 mM [17]. Then, to create gold nanoparticles, combine the obtained solution with 70 mL of boiling gold solution and 1.4 mL of trisodium citrate solution. We utilize a ratio of 1:5 to load bromelain, which means that for every milliliter of bromelain, 5 mL of gold solution are added.

AuNP and Br-AuNP characterization

To measure the absorption spectra, a UV-Vis spectrophotometer (Shimadzu 1900, Japan) operating at room temperature in the 100 - 1,100 nm range was utilized. FTIR spectroscopy (Shimadzu 1800, Japan)

was used to identify the functional groups in solutions at wavelengths ranging from 400 to 4,000 cm^{-1}. Two methods were used to determine the size and shape of the particles: Transmission electron microscopy (TEM) and scanning electron microscopy (SEM). With the use of Philips (PW1730), an X-ray diffraction (XRD) analysis was carried out. Measurements of XRD at a 2θ angle between 20 and 80 ° [18] were made using Cu Kα radiation (λ = 1.54 A). Zeta potential measurement as a means of forecasting the stability of chemically produced gold nanoparticles and bromelain-loaded gold nanoparticles.

Preparation of the carbon tetrachloride solution

To produce the solution, 1 mL of concentrated CCL_4 was diluted with 3 mL of olive oil in a glass beaker. The mixture was then thoroughly mixed and allowed to sit at room temperature until needed [19].

Experimental design and animals

The study comprised 49 male *Mus Musculus* albino mice, aged between 8 and 10 weeks, from Al-Nahrain University's Biotechnology Research Center. Seven mouse groups were present: G1, G2, G3, G4, G5, G6 and G7. G1 was given normal saline on a daily basis, G2 underwent subperitoneal injection of CCl_4 once a week at a concentration of 0.1 mL/100 g of body weight, G3 received an oral dose of Au-Nps solution, and G4 received a subperitoneal injection of CCL_4. An hour later, the mice were given an oral dose of 100 mg/kg bromelain solution at a daily dose of 0.1 mL, and G5 was subperitoneally injected with CCl_4. After 60 min, the mice received the same oral dosage of 100 mg/kg Au-NPs-Bro, G6 and G7 as groups 4 and 5, but with a 300 mg/kg bromelain concentration.

Examinations using histopathology and immunohistochemistry

After removing the kidneys fixed in 10 % concentrated in formalin and washing them under running water, several procedures were carried out by method [20]. A MEIJI light microscope fitted with a high-resolution Canon digital camera was used to take photos of the slides.

Immunohistochemical staining technique Briefly, 4 mm-thick tissue sections were deparaffinized in xylene and hydrated by immersing in a graded ethanol series. Antigen retrieval was performed by using high pH at 95 °C in a water bath for 40 min. Endogenous peroxidase was inhibited by added peroxide black and incubated for 10 min in a humid chamber. A power block was added and incubated for 10 min humid chamber. A power block was added and incubated for 10 min in a humid chamber. The primary antibody was added and incubated for 20 min, the HRP (Horseradish peroxidase) secondary antibody was added and incubated for 10 min Mayer¼s hematoxylin added for 1 min as counter stain, the slides mounted by cover slides and be ready to be examined and do scoring (DAKO, USA).

Analytical statistics

The 1-way ANOVA test was used to find significant differences in the averages using the Statistical Package for the Social Sciences (Version 23) application. The results were presented as (the arithmetic mean ± the standard deviation), with the value of the least significant difference being adopted at the level ($p \leq 0.05$).

Results and discussion

The hue of $HAuCL_4.3H_2O$ changed from light yellow to wine red when a tri-sodium citrate solution was added to chemically prepare the gold nanoparticle solution. This hue shift, as seen in **Figure 1**, is assumed to be the 1st indication that gold nanoparticles are beginning to develop. The color changes of the solutions might have resulted from differences in the electronic density of the nanoparticles driven by variations in their diameters [17]. Surface plasmon resonance (SPR), the product of collective oscillation

of free conduction electrons induced by an interacting electromagnetic field, may account for the visually noticeable color change that indicates the formation of metal nanoparticles [21].

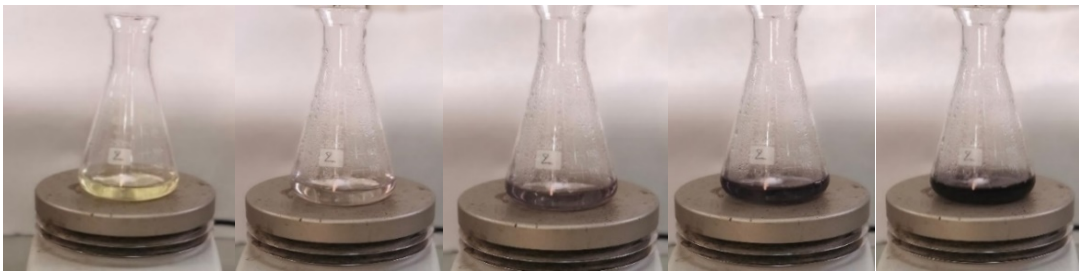

Figure 1 Illustrates how the color changes as gold nanoparticles are produced.

AuNP and Br-AuNP characterization

UV-visible spectrophotometer

Utilizing the results of UV-visible spectroscopy, bromelain conjugation and AuNP synthesis were verified. For Bromelain, AuNPs and AuNPs-Bromelain, respectively, 3 peaks with wavelengths of 276, 534 and 550 nm were seen in **Figure 2**.

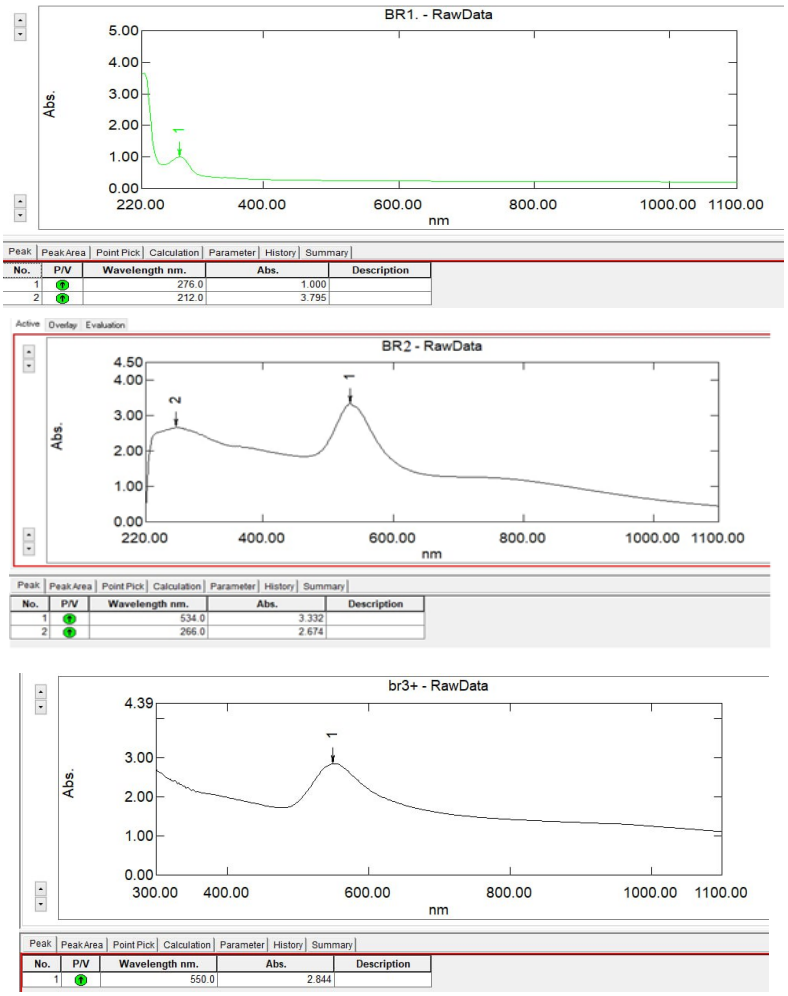

Figure 2 UV-vis analysis of bromelain (BR1), AuNP (BR2) and AuNP-bromelain (BR3).

The wavelengths in issue are indicative of the colloidal spectrum of gold nanoparticles, which confirms the presence of gold and the process of generating gold nanoparticles [22].

Fourier transform infrared spectrometer (FTIR)

One of technique used in this study's characterization part is FTIR. It is used to quantify the intensity of infrared light as a function of frequency or wavelength and to clearly distinguish chemical structures. As seen in **Figures 3(A) - 3(C)**, the FTIR analytical instrument may be utilized to determine functional groups and provide details on covalent bonds. The peaks at frequencies 3,410.18 and 3,653.18, which reflect the findings of the FTIR analysis of the bromelain solution, demonstrate the presence of the OH groups of alcohol and phenol molecules. The FTIR analysis of bromelain Br-AuNP-loaded gold nanoparticles is displayed in **Figure 3(B)**. The absorption peak at frequency 3,305.99 indicates the presence of OH groups in alcohol and phenol, whereas the absorption peak at frequency 1,535.34 indicates the presence of secondary amine and amide groups. A bigger peak at 3,271.27 in the FTIR spectra of the generated AuNPs is characterized as O-H stretching an alcohol band associated with a medium-strong H-bounded vibration, as seen in **Figure 3(C)**. FTIR analysis is used to investigate the adsorption of organic compounds on metal oxide nanoparticles [23]. The results presented here are in line with other research [24,25].

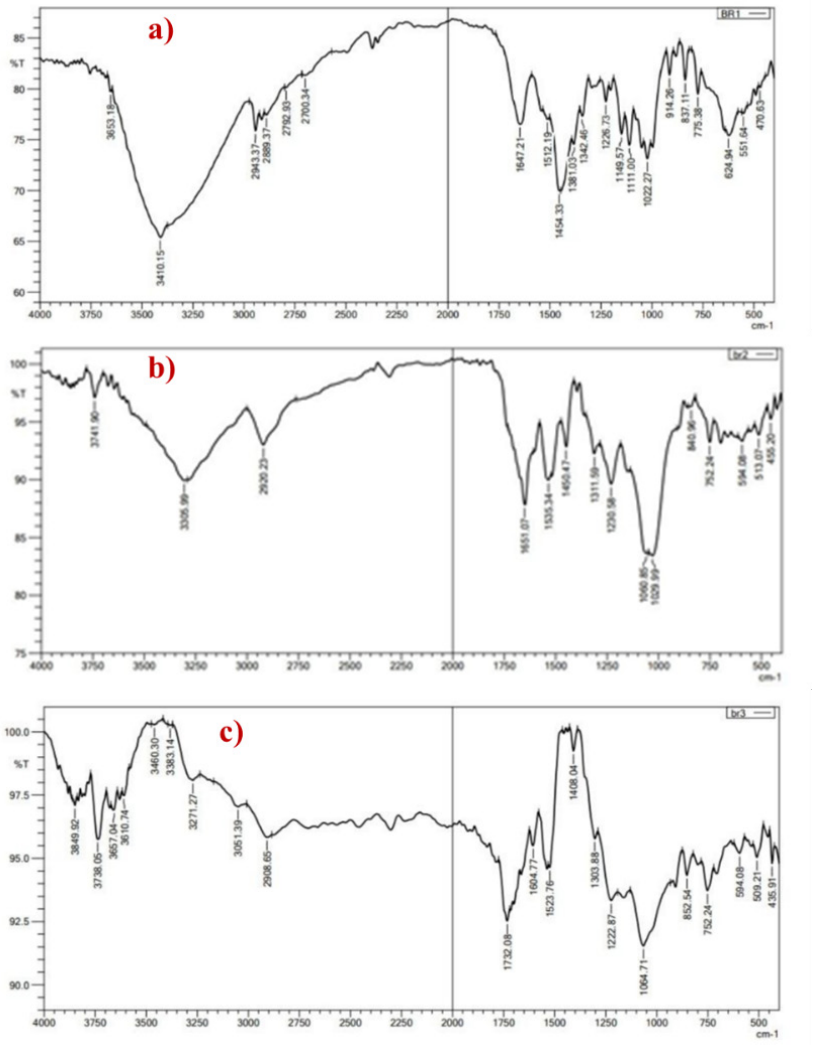

Figure 3 FTIR spectra of (a) Bromelain, (b) AuNPs-Bromelain and (c) AuNPs.

Scanning electron microscopy (FE-SEM) and transmission electron microscopy (TEM)

FE-SEM and TEM pictures of the particle morphology were taken to gain a deeper understanding of the morphological characteristics of AuNPs and AuNPs-Br. AuNPs had an average size of 18 ± 49.36 nm, and **Figures 4(A) - 4(B)** provided FE-SEM images displaying their particle morphologies. Their shape was round and fairly regular. This accounts for the formation of uniformly formed spherical particles. Smooth, well-separated structures were generated by the AuNPs [26,27].

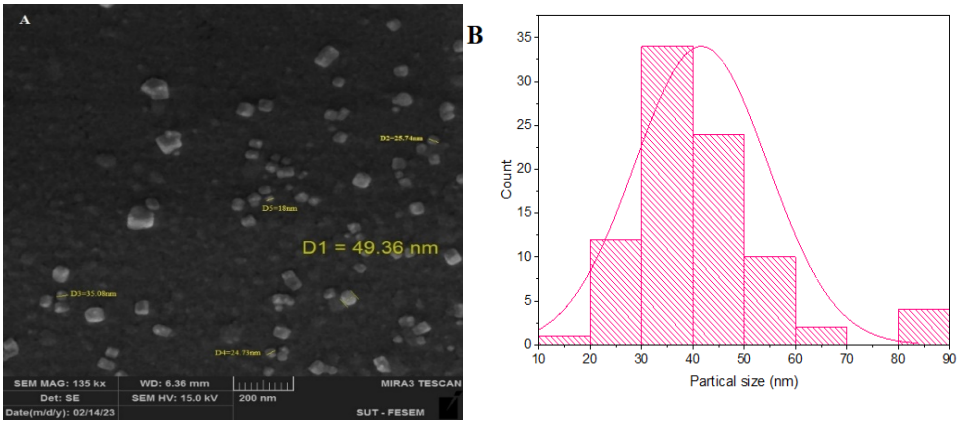

Figure 4 Scanning electron microscopy pictures of (A) AuNPs with a 200 nm scale bar and (B) a histogram of the particle size distribution.

Br-AuNPs morphological characteristics are displayed in **Figures 5(A) - 5(B)**. The gold nanoparticles loaded with Br-AuNPs were shown to have a spherical shape and an uneven distribution of particles with an average size of 46.39 ± 75.39 nm. The findings of this investigation align with those of [27], which created a bromelain-loaded nanolipid formulation intended to treat rheumatoid arthritis.

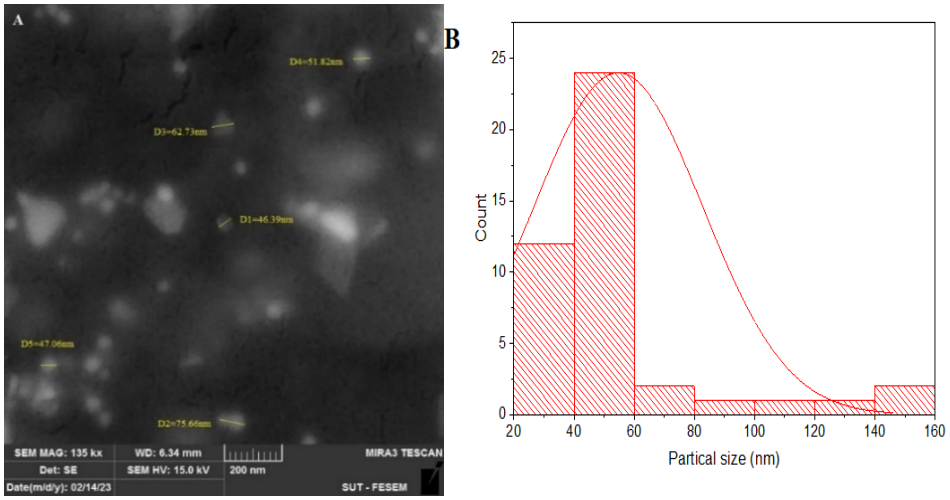

Figure 5 Scanning electron microscopic images for (A) AuNPs -Bromelain with scale bar 200 nm and (B) particle size distribution histogram.

The TEM images of the AuNPs, which have an average size of 7.40 ± 15 nm, are displayed in **Figures 6(A) - 6(B)** and illustrate their well-distributed size and shape. It was noted that the shape of most AuNPs was spherical, this aligns with [28].

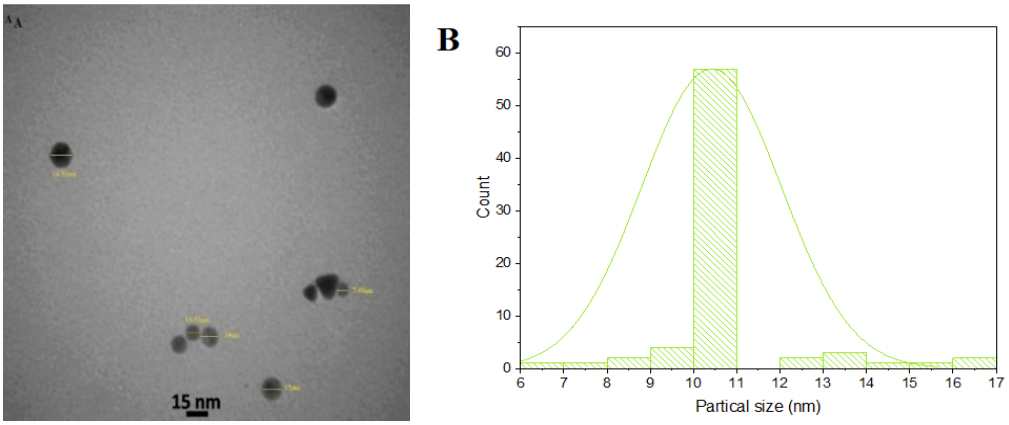

Figure 6 Transmission electron microscopy analysis for (A) AuNPs with scale bar 15 nm and (B) particle size distribution histogram.

Research examining the surface morphology of Br-AuNPs produced spherical particles with a size of 43.05 ± 110 nm. Some nanostructures (**Figures 7(A) - 7(C1)**) have sharp edges and triangular forms. According to reference [27], the TEM image of Br-AuNPs revealed that they were quite large, indicating that the bromelain had adhered to the AuNP surface.

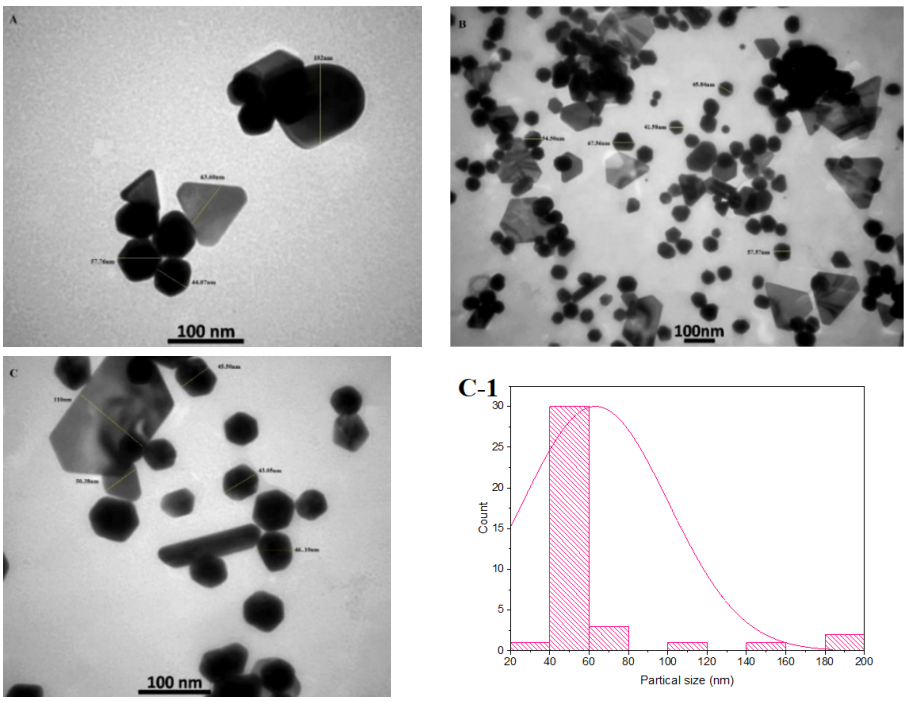

Figure 7 (A) - (D) Transmission electron microscopy analysis for (A) - (C) AuNPs-Bromelain with scale bar 100 nm, (C-1) particle size distribution histogram.

Zeta potentials

Zeta potentials (ZP) of gold nanoparticle bioconjugates (AuNP-bios) provide important surface charge information for drug delivery, biosensing, and cell imaging, among other applications. High-frequency ZP measurements (ZPMs) are performed in an alternative electrical field. AuNPs-Bromelain was discovered to have a zeta potential of +1.2 ± 3.0 mV, which is much less than that of unconjugated Au-

NPs, which showed a zeta potential of +0.1 ± 0.4 mV. Given that conjugation includes the addition of extra carboxylic groups, this suggests that there was no agglomeration of nanoparticles following the procedure. The results of this study are consistent with the results of the earlier study [29].

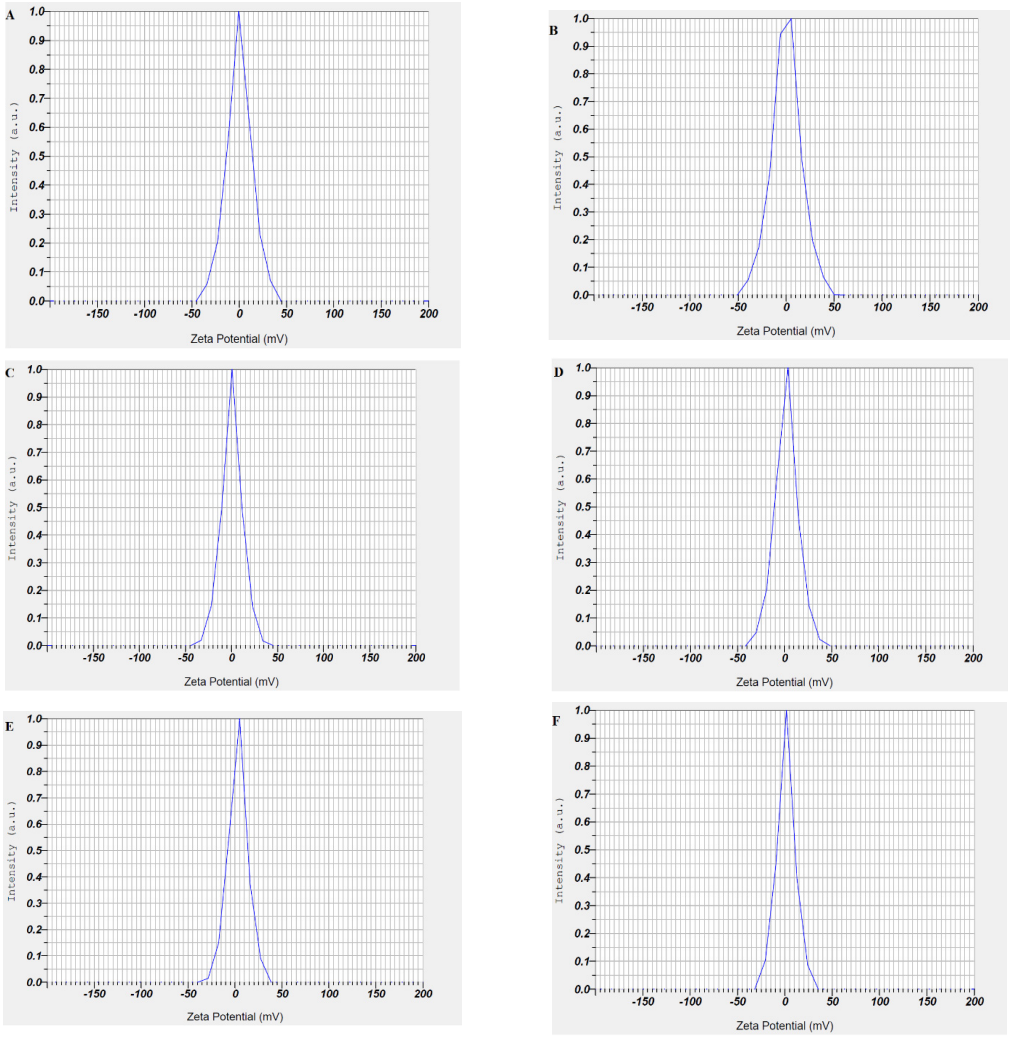

Figure 8 Zeta potential analysis (A) - (C) AuNPs and (D) - (F) AuNPs-Bromelain.

X-ray diffraction

X-ray diffraction (XRD) examination was utilized to investigate the crystalline phases of AuNPs and AuNPs-bromelain, as shown in **Figures 9(A) - 9(B)**, to determine phase purity and crystal structure. With JCPDS data file No. 04-0784 as a standard reference, it was determined that the synthesized gold nanoparticles under examination produced consistent findings when analyzed using X-ray diffraction spectroscopy at an angle of 20. This implies that the crystalline nature of the produced gold nanoparticles is present. Face-centered cubic structures are common in crystalline structures. XRD pattern revealed that AuNPs (**Figure 9(A)**) were produced by chemical reduction after Au3+ was completely reduced to Au0. The observed diffraction peaks at 111.84, 200.31, 202.98 and 311.55 ° are in agreement with the acquired strong peaks (JCPDS, USA) for the standard gold metal (Au0). The results indicate a high degree of agreement with several earlier research investigations [30-32]. As seen in **Figure 9(B)**, the difference between the XRD peaks of AuNPs and AuNPs-bromelain shows that bromelain and AuNPs have coupled to create AuNPs-bromelain. The investigation's findings demonstrated that bromelain loading did not affect

the crystal structure of silver nanoparticles. The additional peaks in the X-ray diffraction analysis, according to study [33] are caused by biomolecules, such as phytochemical components, that are present on the surface of the nanoparticles. In some samples, stabilizing factors like proteins and enzymes can also cause these peaks.

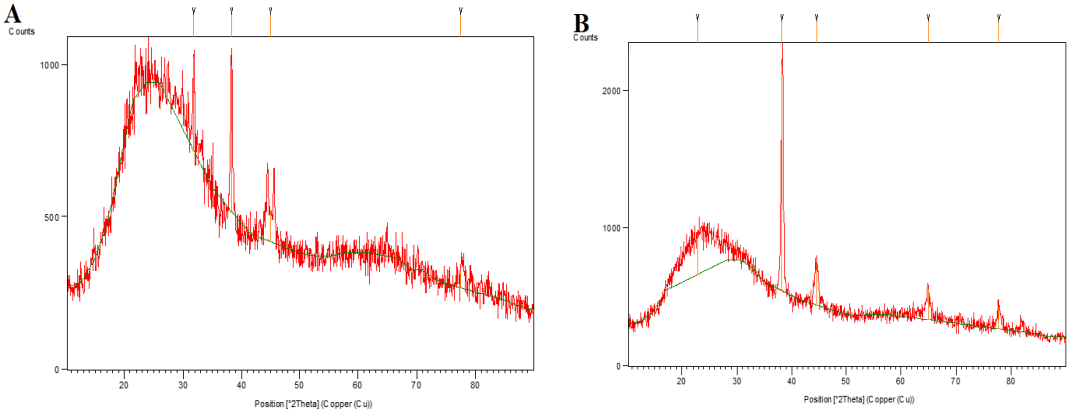

Figure 9 The XRD patterns, (A) AuNPs and (B) AuNPs-bromelain.

Histopathological study

Comparing the kidney sections from albino mice to the control group revealed variations in the capacity of bromelain solution and AuNPs-Bro to completely remove the harmful effects of carbon tetrachloride. The control group showed normal cytoarchitecture of glomeruli and renal tubules (**Figure 10(A)**). The 2nd group showed degeneration of renal tubules and focal interstitium thickening associated with congestion and infiltration of leukocytes (**Figure 10(B)**). The 3rd group showed revealed mild renal congestion, and the magnified figures showed mild vascular congestion of glomerular tufts, mild tubular cast formation and little inflammatory infiltration (**Figure 10(C)**). The 4th group revealed a normal appearance of glomeruli with mild vascular congestion, per vascular lymphocytic cuffing and normal interstitium (**Figure 10(D)**). The 5th group revealed the normal appearance of the cytoarchitecture of glomeruli, renal tubules and renal interstitium (**Figure 10(E)**). The 6th group revealed that the renal cortex and medulla showed marked glomerular congestion with severe vascular degeneration with necrosis of lining cells of all segments of renal tubules (**Figure 10(F)**). The 7th group showed the renal cortex and the medulla showed normal glomeruli and segments of renal tubules (**Figure 10(G)**).

In this investigation, renal damage was induced by administering CCl_4, a hepatotoxin and nephrotoxin that has also been demonstrated to have toxic effects on the kidney in addition to the liver [34,35]. These papers claim that the cytochrome P450 enzyme converts CCl_4 to CCl_3 and CCl_3O_2, which causes CCl_4-induced liver damage. Cell damage is brought on by these very reactive free radicals. However, it is still unclear how CCl_4 causes kidney damage [36]. The kidney examination of the prebiotic and carbon tetrachloride group proved the renal-protective effect of prebiotics on the nephrotoxicity of carbon tetrachloride. Ozturk *et al.* [35] discovered that pretreatment with betaine reduced the substantial glomerular and tubular changes in the renal cortex that were widely generated by subcutaneous injections of CCl_4 to rats at daily dosages of 1 mL/kg for 7 days. According to Doğukan *et al.* [34], continuous treatment of CCl_4 (0.15 mL/kg, sc, in olive oil) for 7 weeks at a time in rats resulted in varying degrees of tubular and glomerular alterations, interstitial mononuclear cell proliferation and kidney fibrosis.

Due to its anti-inflammatory effects, bromelain delivery along with CCL_4 improved lipids and protein levels. This is consistent with [37] studies in rats treated with high doses of lead-generated dyslipidemia,

which was relieved by stem bromelain therapy. Due to its antioxidant action, administration of bromelain protects kidney function biomarkers as well as enzyme activities from CCl_4-intoxication as demonstrated by a considerable restoration compared to the CCl_4 treated group.

While bromelain had a protective effect at high dosages of 100 and 300 mg, the present study found that mice injected with a bromelain solution loaded with gold nanoparticles exhibited a superior protective effect.

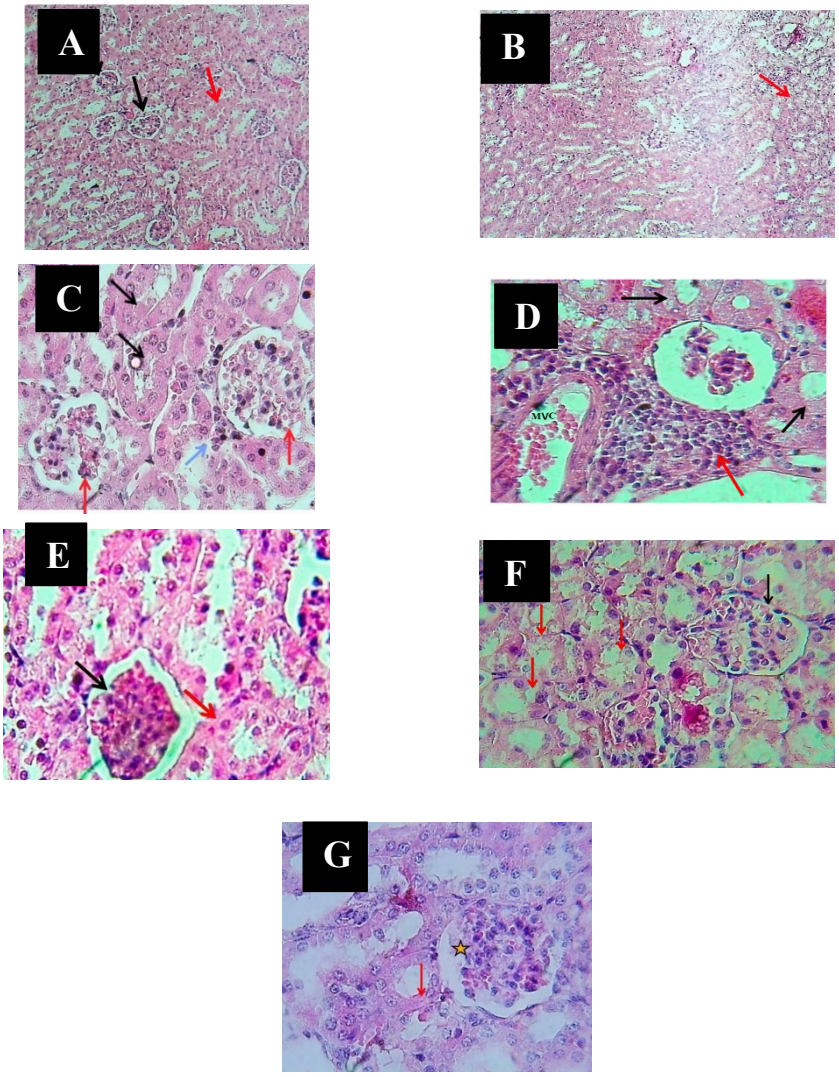

Figure 10 (A) normal appearance of glomeruli (red arrows), renal tubules (black arrow) and normal interstitum, H & E 400×. (B) degeneration of renal tubules (red arrows) and focal interstitum thickening associated with congestion and infiltration of leukocytes (black arrow), H & E stain 40×. (C) mild vascular congestion of glomerular tufts (red arrows), mild tubular cast formation (black arrows) and little inflammatory infiltration (blue arrow). (D) normal appearance of renal tubules (black arrow), mild vascular congestion (MVC), and per vascular lymphocytic cuffing (red arrow). (E) normal glomerulus (red arrows), and normal tubules (red arrows). (F) congested glomerulus (black arrow) and vascular degeneration of lining epithelial cells of renal tubules (red arrows), H & E stain 400×. (G) shows normal glomerulus (black arrow) and normal renal tubules (red arrow), H & E stain 100×.

Immunohistochemical study

Caspase-9 immunohistochemical results in kidney

The immunohistochemical study showed the cell membrane of kidney tissue sections of mice positive expression of caspase-9 with varying intensity, with a weak score of +2 for control animals negative and varying scores +2 - +3 in other treatment totals **Table 1**.

The present study focused on the assessment of Au-NPs-Bro treatment outcomes for treating CCl_4-induced nephropathy, by evaluating kidney functions, caspase-9. The current *in vivo* study treatment of CCl_4 produced nephropathy, as evidenced by modifications to biochemical parameters, histological alterations and molecular expression changes. One important role that caspases, a class of proteases, perform in programmed cell death [38]. CCl_4 caused oxidative stress, on the mitochondria. This stress enhanced the intrinsic route of apoptosis by upregulating the expression of Bcl2 mRNA and reducing the level of caspase-9 mRNA [39].

The results of [40] investigation showed that, when CCl_4 (GPIII) was used instead of GPI to stimulate Bcl-2 mRNA expressions in rat liver and kidney tissue, the expression of caspase 9 mRNA was higher in GPIII than in GPI. The reduction in Bcl-2 expression mRNA stimulates the release of cytochrome c from mitochondria into the cytosol, which stimulates the expression of caspase-9 mRNA regulation for activating apoptotic processes through the liver and kidney tissue's cytoplasm and membranes.

In comparison to the control group, there was an increase in caspase-9 expression in the groups that received doses of carbon tetrachloride, gold nanoparticle solution and 100 mg of bromelain solution. These observations suggest that apoptosis was present. The study's findings showed that the groups who received a 300 mg dosage of bromelain solution had a decrease in apoptosis.

Table 1 Expression of caspase-9 in all the cells except the nucleus of kidney tissue of albino mice.

Groups	Score of Caspase-9	
Control group	+2 N	all the cells except the nucleus
CCL_4 solution	+3 N	all the cells except the nucleus
Gold nanoparticles solution	+3	all the cells except the nucleus
CCL_4 + Bromelain 100 mg	+2	all the cells except the nucleus
CCL_4 + Bromelain 100 mg loaded with the nanoparticles	+3	all the cells except the nucleus
CCL_4 + Bromelain 300 mg	+2	all the cells except the nucleus
CCL_4 + Bromelain 300 mg loaded with the nanoparticles	+2	all the cells except the nucleus

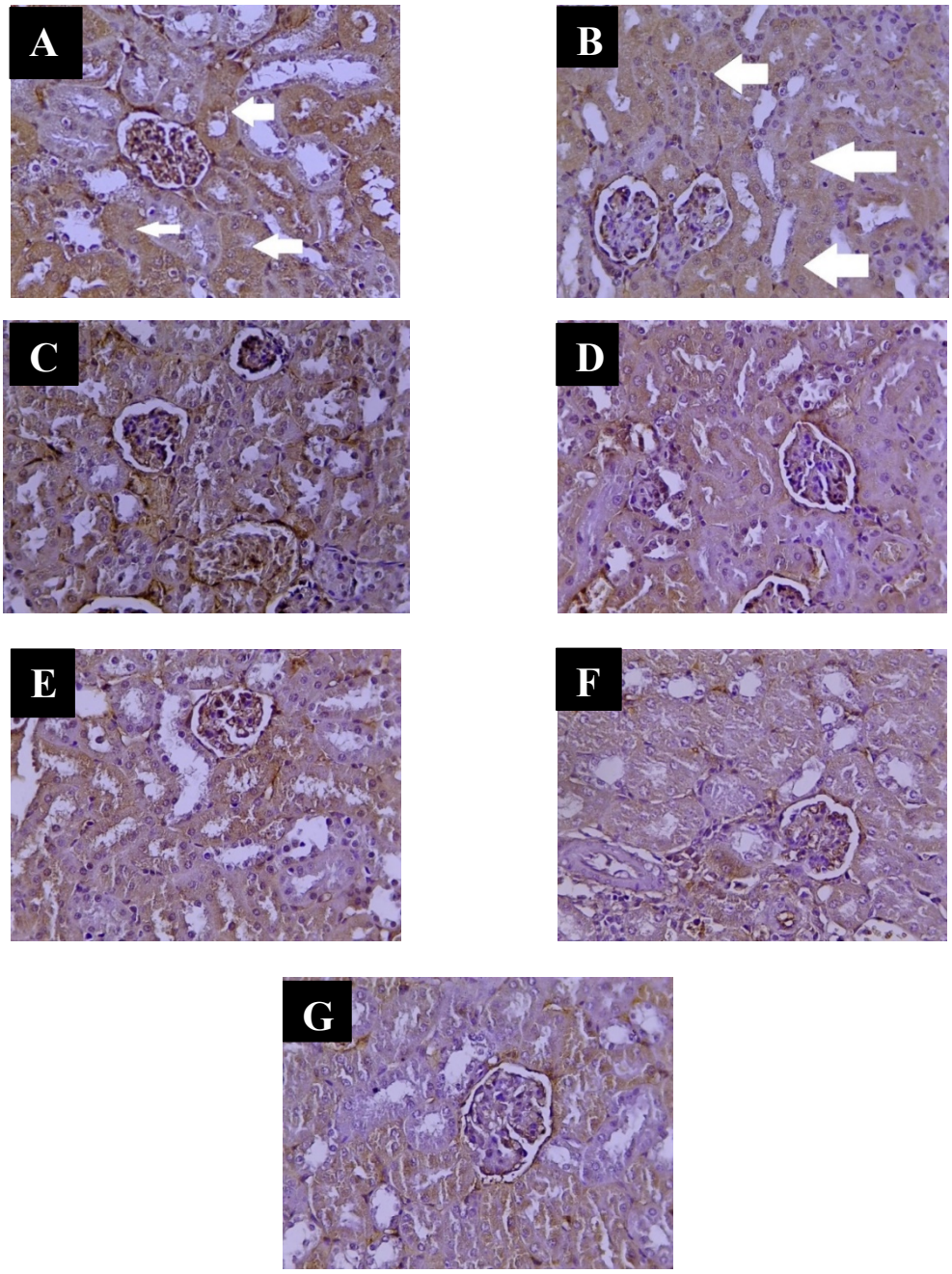

Figure 11 (A) section of the kidney control showed positive (+3) (black arrow) (IHC.40X) (G1). (B) section of the kidney control showed positive caspase-9 (+3) (black arrow) (IHC.40X) (G2). (C) section of the kidney treated by AuNps showed (IHC) score (+3) (IHC.40X) (G3). (D) section of the kidney treated by CCL_4 + Bromelain 100 mg showed (IHC) score (+2) (IHC.40X) (G4). (E) section of the kidney treated by CCL_4 + Bromelain 100 mg loaded gold nanoparticles showed (IHC) score (+3) (IHC.40X) (G5). (F) section of the kidney treated by CCL_4+Bromelain 300 mg showed (IHC) score (+2) (IHC.40X) (G6). (G) section of the kidney treated by CCL_4+Bromelain 300 mg loaded gold nanoparticles showed (IHC) score (+2) (IHC.40X) (G7).

Conclusions

The findings of this study suggest that kidney damage from carbon tetrachloride can occur through oxidative stress, altering the antioxidant defense system, enzyme function and biochemical markers. Therefore, by improving the state of the antioxidant defense system and reducing the production of free radicals, bromelain dramatically decreased the toxicity of CCL_4. For rats given carbon tetrachloride injections, the 300 mg bromelain solution proved more efficacious than the 100 mg dose. The microscopic studies revealed that the treatment with bromelain Loaded on AuNPs has been shown to reduce cellular damage in the liver and kidney of albino mice tissues.

Acknowledgments

Many thanks to the Department of Biology, College of Education for Pure Science (Ibn Al-Haitham), University of Baghdad for facilitating the work of the practice parts in this article.

References

[1] F Provincial. *Guidelines for Canadian drinking water quality: Guideline technical document - carbon tetrachloride*. Health Canada, Ottawa, Cananda, 2010.

[2] KJ Lee, ER Woo, CY Chio, DW Shin, DG Lee, HJ You and HG Jeong. Protective effect of octreotide on carbon tetrachloride-induced hepatotoxicity. *Life Sci.* 2004; **74**, 1051-64.

[3] YM Abd-Elhakim, MH Ghoneim, LLM Ebraheim and TS Imam. Taurine and hesperidin rescue carbon tetrachloride-triggered testicular and kidney damage in rats via modulating oxidative stress and inflammation. *Life Sci.* 2020; **254**, 117782.

[4] J Koh, SM Kang, SJ Kim, MK Cha and YJ Kwon. Effect of pineapple protease on the characteristics of protein fibers. *Fibers Polym.* 2006; **7**, 180-5.

[5] C Chaisakdanugull, C Theerakulkait and RE Wrolstad. Pineapple juice and its fractions in enzymatic browning inhibition of banana (Musa (AAA Group) Gros Michel). *J. Agr. Food Chem*. 2007; **55**, 4252-7.

[6] BN Tochi, Z Wang, SY Xu and W Zhang. Therapeutic application of pineapple protease (bromelain): A review. *Pak. J. Nutr.* 2008; **7**, 513-20.

[7] A Manosroi, C Chankhampan, K Pattamapun, W Manosroi and J Manosroi. Antioxidant and gelatinolytic activities of papain from papaya latex and bromelain from pineapple fruits. *Chiang Mai J. Sci.* 2014; **41**, 635-48.

[8] M Al-Jubori, AA Hassan and R Al-Bahrani. Evaluation of antioxidants for Agaricus bisporus and different strains of *Pleurotus ostreatus*. *Iraqi J. Sci.* 2023; **57**, 316-24.

[9] SI Hussein, AF Kaluf, Y Ahmed, B Ahmed and A Iyad. Determination of inhibition activity of α-amylase enzyme, antioxidant activity, antibacterial activity, and phenolic compounds by using some medical plants. *Iraqi J. Agr. Sci.* 2020; **51**, 411-21.

[10] IS Young and JV Woodside. Antioxidants in health and disease. *J. Clin. Pathol.* 2001; **54**, 176-86.

[11] TA Muhsen, SN Hawar, TS Mahdi and R Khaleel. Effect of Eucalyptus and Myrtus extracts identification by gas chromatography-mass spectrometry on some species of Candida as a model of medical plants. *Ann. Trop. Med. Public Health* 2020, https://doi.org/10.36295/ASRO.2020.231032.

[12] E Abdalrazaq, AAQ Jbarah, TH Al-Noor, GT Shinain and MM Jawad. Synthesis, DFT calculations, DNA interaction, and antimicrobial studies of some mixed ligand complexes of oxalic acid and Schiff base Trimethoprim with various metal ions. *Indones. J. Chem.* 2022; **22**, 1348-64.

[13] SI Hussein, SS Shubber and NY Yaseen. Bio-distribution of gold nanoparticles in tumor mass and different organs in implanted mice with mammary adenocarcinoma AM3 (*in vivo* study). *Iraqi J. Vet. Med.* 2019; **43**, 17-22.

[14] Z Li, N Song and YW Yang. Stimuli-responsive drug-delivery systems based on supramolecular nano valves. *Matter* 2019; **1**, 345-68.

[15] O Schickling, AH Stegh, J Byrd and ME Peter. Nuclear localization of DEDD leads to caspase-6 activation through its death effector domain and inhibition of RNA polymerase I-dependent transcription. *Cell Death Differ.* 2001; **8**, 1157-68.

[16] JB Denault and GS Salvesen. Caspases: Keys in the ignition of cell death. *Chem. Rev.* 2002; **102**, 4489-500.

[17] AK Khan, R Rashid, G Murtaza and A Zahra. Gold nanoparticles: Synthesis and applications in drug delivery. *Trop. J. Pharm. Res.* 2014; **13**, 1169-77.

[18] HAS Al-Shmgani, WH Mohammed, GM Sulaiman and AH Saadoon. Biosynthesis of silver nanoparticles from *Catharanthus roseus* leaf extract and assessing their antioxidant, antimicrobial, and wound-healing activities. *Artif. Cells Nanomed. Biotechnol.* 2017; **45**, 1234-40.

[19] BS Abeed and HA Al-Shmgani. Evaluation of the potential protective role of Galangin associated with gold nanoparticles in the histological and functional structure of testes of adult male albino mice administrated with carbon tetrachloride. *Baghdad Sci. J.* 2024, https://doi.org/10.21123/bsj.2024.9086.

[20] A Stevens and JD Bancroft. *Theory and practice of histological techniques*. Churchill Livingston, London, 2010.

[21] P Mulvaney, M Giersig and A Henglein. Electrochemistry of multilayer colloids: Preparation and absorption spectrum of gold-coated silver particles. *J. Phys. Chem.* 1993; 97, 7061-4.

[22] HH Al-Salhie and EJ Al-Kalifawi. Antimicrobial and antivirulence activity of magnesium oxide nanoparticles synthesized using *Klebsilla pneumonia* culture filtrate. *Biochem. Cell. Arch.* 2020; **20**, 3991-4001.

[23] RK Tekade. *Biomaterials and bionanotechnology*. Elsevier, London, 2019.

[24] AM Mohammed and MT Sultan. Synthesis, characterization and biological activities of new nano Schiff bases composites. *Ibn Al Haitham J. Pure Appl. Sci.* 2020; **33**, 55-67.

[25] AJ Abdulghani and SK Mohuee. Synthesis of gold nanoparticles using ceftriaxone sodium as a reducing and stabilizing agent. *Iraqi J. Sci.* 2015; **56**, 2425-38.

[26] SN Hawar, HS Al-Shmgani, ZA Al-Kubaisi, GM Sulaiman, YH Dewir and JJ Rikisahedew. Green synthesis of silver nanoparticles from *Alhagi graecorum* leaf extract and evaluation of their cytotoxicity and antifungal activity. *J. Nanomater.* 2022; **2022**, 1058119.

[27] AHA Dujaily and AK Mahmood. The effectiveness of biogenic silver nanoparticles in the treatment of caprine mastitis induced by *Staphylococcus aureus*. *Iraqi J. Vet. Sci.* 2021; **35**, 73-8.

[28] M Sharma and D Chaudhary. Exploration of bromelain laden nanostructured lipid carriers: An oral platform for bromelain delivery in rheumatoid arthritis management. *Int. J. Pharmaceut.* 2021; **594**, 120176.

[29] B Marie. 2017, Synthesis, physicochemical characterisation and biological evaluation of polymer-functionalised gold nanoparticles for cancer treatment. Ph.D. Dissertation. Imperial College London, London, England.

[30] HH Qasim, HA Abdullah and AR Mujahid. Effect of *Olea europea* L extraction and TiO2 nanoparticles against *Pseudomonas aeruginosa*. *Indian J. Publ. Health Res. Dev.* 2019; **10**, 1218-23.

[31] HS Hakeem and NK Abbas. Preparing and studying structural and optical properties of Pb1-xCdxS nanoparticles of solar cells applications. *Baghdad Sci. J.* 2021; **18**, 640.

[32] MHA Latif and YF Mahmood. Isolation and characterization of microcrystalline cellulose and preparation of nano-crystalline cellulose from tropical water hyacinth. *Ibn Al Haitham J. Pure Appl. Sci.* 2018; **31**, 180-8.

[33] R Debnath, DD Purkayastha, S Hazra, NN Ghosh, CR Bhattacharjee and J Rout. Biogenic synthesis of antioxidant, shape selective gold nanomaterials mediated by high altitude lichens. *Mater. Lett.* 2016; **169**, 58-61.

[34] A Doğukan, N Akpolat, H Celiker, N Ilhan, IH Bahçecioğlu and AI Günal. Protective effect of interferon-alpha on carbon tetrachloride-induced nephrotoxicity. *J. Nephrol.* 2023; **16**, 81-4.

[35] F Ozturk, M Ucar, IC Ozturk, N Vardi and K Batcioglu. Carbon tetrachloride-induced nephrotoxicity and protective effect of betaine in Sprague-Dawley rats. *Urology* 2003; **62**, 353-6.

[36] G Venkatanarayana, G Sudhakara, P Sivajyothi and P Indira. Protective effects of curcumin and vitamin E on carbon tetrachloride-induced nephrotoxicity in rats. *EXCLI J.* 2012; **11**, 641-50.

[37] WR Al-Otaibi, P Virk and M Elobeid. Ameliorative potential of stem bromelain on lead-induced toxicity in Wistar rats. *Acta Biologica Hungarica* 2015; **66**, 149-60.

[38] KJ Livak and TD Schmittgen. Analysis of relative gene expression data using real-time quantitative PCR and the 2(-Delta Delta C(T)) method. *Methods* 2001; **25**, 402-8.

[39] JD Bancroft and GA Stevens. *Theory and practice of histological techniques*. Churchill Livingstone, London, 1990.

[40] RM Mainardes and RC Evangelista. PLGA nanoparticles containing praziquantel: Effects of formulation variables on size distribution. *Int. J. Pharmaceut.* 2005; **290**, 137-44.